Environmental Processes (2021) 8:287–310
https://doi.org/10.1007/s40710-020-00471-2

ORIGINAL ARTICLE

# Modification of *Adansonia digitata* Cellulose by Hydroxamic Acid: a Promising Resource for Removing Pb (II) Ions from Water

**Adewale Adewuyi** [1]

Received: 17 June 2020 / Accepted: 29 September 2020/ Published online: 6 October 2020


**Abstract**
Developing cheap and affordable materials for the removal of toxic heavy metal ions such as Pb (II) ions from water is a challenge. In response to this, this work evaluated the synthesis and use of hydroxamic acid modified *Adansonia digitata* cellulose (ADHX) as a useful resource for the removal of Pb (II) ions from water. ADHX was characterized using Fourier Transform Infrared spectrometry (FTIR), Thermogravimetric analysis (TGA), X-ray Diffraction analysis (XRD), zeta potential, Particle Size Dispersion (PSD), Scanning Electron Microscopy (SEM) and Energy Dispersive Spectroscopy (EDS). The sorption of Pb (II) ions on ADHX follows the pseudo-second order model, intra-particle diffusion and Liquid film diffusion kinetic models. The adsorption capacity of ADHX was found to be 18.00 mg $g^{-1}$, which fitted well for Langmuir, Temkin and Freundlich isotherms. PSD revealed ADHX to be monomodal while Gibb's free energy change ($\Delta G^o$) suggests a non-spontaneous process. The negative nature of enthalpy change ($\Delta H^o$, −69.774 kJ $mol^{-1}$) shows that the process is exothermic while entropy change ($\Delta S^o$, −0.214 kJ $mol^{-1}$) suggests a stable configuration of Pb (II) ions on the surface of ADHX. However, the desorption studies revealed a possible regeneration of ADHX with a desorption capacity of 68.75% in 0.01 M $NaNO_3$ while quantum chemical computation using Density Functional Theory (DFT) revealed the mechanism of sorption to be via ionic interaction. This study revealed ADHX to be a promising resource for removing Pb (II) ions from water.

**Keywords** *Adansonia digitate* · Adsorption · Biosorbent · Heavy metal · Isotherm

✉ Adewale Adewuyi
walexy62@yahoo.com

[1] Department of Chemical Sciences, Faculty of Natural Sciences, Redeemer's University, Ede, Osun state, Nigeria

## 1 Introduction

Water pollution by chemical compounds is an environmental challenge. The pollution may be caused by human activities, which leads to the generation of domestic and industrial wastes. When these wastes get into the environment, they become pollutants, especially when they get into the water system. Some of these are responsible for the pollution of surface and groundwater in several countries of the world, particularly in developing countries like Nigeria. Pollution of surface and groundwater makes access to clean drinking water difficult. Contamination of rivers and streams in developing countries is a common problem, which makes the provision of potable drinking water a challenge. An effort has been made in the past to mitigate contamination by employing different techniques like oxidation, filtration, adsorption, catalysis, electrochemistry, photo-degradation and phytoremediation (Merganpour et al. 2015; Babu et al. 2016; Zhao et al. 2016; Ravulapalli and Kunta 2017); however, these approaches have shortcomings such as insufficient removal of pollutants, high-energy requirement, making them expensive and unsustainable. Among the known methods, adsorption remains one of the most promising methods for the removal of pollutants in water because it is inexpensive and can be easily modified.

Several chemical pollutants have been identified in water (Triantafyllidou and Edwards 2012; Koesmawati et al. 2017; Wasike et al. 2019) but the inorganic ones are of serious concern in most African countries like in Nigeria (Orosun et al. 2016; Tenebe et al. 2018). Pb is one of the inorganic pollutants found in water. Different concentrations of Pb have been reported in water systems, which ranges from 100 to 1000 ppm (Galadima et al. 2010; Galadima and Garba 2012; Oke et al. 2017). Several conditions have contributed to the concentrations reported, such as activities in industries like battery, mining and metallurgic, metal sheet, paint, and trash incineration. The presence of Pb has been reported in water sources in both developed and developing nations (Anyanwu et al. 2018; Bolisetty et al. 2019; Joseph et al. 2019). Most industries generating Pb in their waste needs to properly treat the wastes so that Pb does not get into the environment. Presence of Pb in water bodies such as river, lake, groundwater and the ocean is a big concern in developing countries such as Nigeria. Continuous exposure to Pb is dangerous, which may result in serious health problems such as learning disability, and damage to the brain, the nervous system and the liver (WHO 2010). As local industries are emerging and developing, there is a need to develop techniques for the treatment of effluents from these industries. Currently, most small scale local industries in very low-income nations do not have an efficient technique that can completely remove heavy metals like Pb from effluents because some of the efficient techniques are expensive, not easily set-up and difficult to sustain. This has necessitated the need to develop a technique that is cheap, efficient and easy to use. Previous studies have reported the use of a variety of adsorbents such as synthetic mineral (Chen and Shi 2017) and molybdenum sulfide ($MoS_2$)/thiol-functionalized multiwalled carbon nanotube (Gusain et al. 2019). One major challenge with the use of synthetic mineral is the technical viability mostly when treating large volume of polluted water with metal ions. Composite materials using polymers and adsorbents have also been used (Abdeen 2015). Such composite may include the elastomeric polyurethane foam as matrix materials to support adsorbents like zeolite and activated carbon. However, the use of such composite is limited due to difficulties in separating the adsorbed metal ions from the composite

materials making it difficult to regenerate the composite material for further use (Choi and Jeong 2008; Abdeen 2015). Use of nanomaterials has the challenge of sludge generation, toxicity and high operation cost. The main drawbacks of the aforementioned techniques are lack of sustainability and high operation costs, most especially when the concentration of Pb ions is below 100 mg $L^{-1}$ (Escudero-Oñate et al. 2017). However, the use of biosorbent has shown much encouragement. Reported biosorbents includes ion-imprinted magnetic biosorbent (He et al. 2019), modified residues of *Anacardium occidentale* L (Coelho et al. 2018), *Jatropha curcas* (Nacke et al. 2016), and *Moringa oleifera* biomass (Imran et al. 2019). Most biosorbents are plant-sourced, which shows they are from a renewable source with low toxicity. They are biodegradable, which is an advantage over synthetic materials from petrochemicals. Cellulose is a plant-sourced material that can be used as a biosorbent.

Cellulose is a linear chain polymer with β-D-glucopyranose units joined by β-1, 4 glycosidic linkages. It is insoluble in water and biodegradable. It is a semi-crystalline polymer with methylol and hydroxyl functional groups. It has both crystalline and amorphous phases. The presence of hydroxyl functional group in its molecule is an indication that it can be modified to improve on its properties. It contains two types of hydroxyl groups, primary hydroxyl in the methylol group (-$CH_2OH$) at C-6 and secondary hydroxyl groups (-OH) at C-3 and C-4 (Hokkanen et al. 2016). A few modifications of cellulose have been reported such as etherification (Fox et al. 2011), oxidation (Batmaz et al. 2014) and esterification (Yu et al. 2013). It is evident that simple modification of cellulose may overcome the present challenge facing the removal of Pb ions in water. Modifying the surface of cellulose may improve some of its properties such as mechanical strength, thermal stability, hydrophobicity and elasticity, which may enhance its adsorption capacity towards Pb ions and other toxic heavy metal ions. Cellulose based material is eco-friendly, low-cost, readily available and may become selective towards target Pb ions in water when modified (Sarkar and Sarkar 2017). Buvaneswaria and Kannanb (2011) have shown that cellulose modified with glycidyl methacrylate and diethylenetriaminepentaacetic acid exhibited encouraging regeneration capacity when used for the adsorption of green and basic fuchsin dye malachite. Despite this success, the use of cheap and simple chemicals to achieve impressive modification for removal of toxic metals in water is limited. The study aim at achieving this by proposing the use of hydroxamic acid for improving the property of cellulose. Hydroxamic acid is an amide where the NH centre group has OH substituent. The aim is to improve on the capacity of cellulose as a biosorbent for the removal of Pb (II) ions in solution. The use of hydroxamic acid as a modifying agent will introduce amide group on the cellulose with the presence of heteroatoms that can interact with Pb (II) ions in solution.

Despite the role of cellulose as biosorbent, many studies have focused on the preparation of cellulose nanocomposite, which ended up being expensive and with low regeneration capacity as well as sludge generation. However, this study capitalizes on imprinting the amide group on cellulose as a source of nonbonding electron that can specifically interact with Pb ions in solution with the aim of cost reduction with improved regeneration capacity. To achieve this, cellulose isolated from *Adansonia digitata* was modified with hydroxamic acid to improve on the efficiency of cellulose as a biosorbent for the removal of Pb (II) ions from the water.

## 2 Material and Methods

### 2.1 Materials

Seeds of *Adansonia digitata* were collected from the Botanical garden at the University of Ibadan, Nigeria. The seeds were defatted by extraction with n-hexane in a soxhlet extractor (Adewuyi et al. 2012). Chloroacetic acid, thionyl chloride, sodium hydroxide, sodium chlorite, glacial acetic acid, sodium sulphate, ethyl acetate, hydroxylamine hydrochloride, n-hexane and all other chemicals were purchased from Sigma-Aldrich (Brazil). Stock solutions of Pb (II) ions were prepared by dissolving an appropriate amount of $Pb(NO_3)_2$ in deionized water in 1000 mL standard flask. The stock solution was diluted with deionized water to prepare different experimental solutions.

### 2.2 Isolation of Cellulose from the Defatted Seed of *Adansonia digitata*

The isolation of cellulose from the defatted seed of *Adansonia digitata* was achieved as previously described by Flauzino Neto et al. (2013). Briefly, 2% NaOH was added to a 5 L beaker containing the defatted seed of *Adansonia digitate*, stirred for 5 h at 80 °C. The filtrate obtained was washed with distilled water until alkali free. The filtrate was bleached with a reagent containing acetate buffer and aqueous sodium chlorite in ratio 1:1. This was stirred continuously at 80 °C for 5 h. It was washed continuously with distilled water until the residue became pH neutral. The bleaching step was repeated three more times until the product was completely white. Cellulose obtained was dried at 60 °C for 24 h.

### 2.3 Synthesis of Hydroxamic Acid from the Seed Oil of *Adansonia digitata*

Hydroxamic acid was prepared using the oil extracted from the seed of *Adansonia digitata* during defatting. The synthesis has been previously reported (Adewuyi et al. 2019). Briefly, synthesis was achieved by first converting the seed oil to methyl esters at 70 °C using 1% KOH as catalyst, followed by hydroxylation using formic acid (0.0106 mol) and hydrogen peroxide (0.407 mol), and finally, reacting the hydroxylated methyl esters with hydroxylamine hydrochloride in the presence of sodium methoxide as a catalyst. The product was characterized by FTIR and $^1$HNMR as reported (Adewuyi et al. 2019).

### 2.4 Preparation of ADHX

Thionyl chloride (0.04 mol) and chloroacetic acid (0.03 mol) were mixed in chloroform in a 500 mL three-neck round bottom flask at 75 °C for 30 min (Fig. 1a). The isolated *Adansonia digitata* cellulose (5.00 g) was added to the mixture while heating and stirring at 80 °C for 3 h. This was cooled in ice while removing the excess reagent. Hydroxamic acid (0.04 mol) was added to the residue left in the round bottom flask while stirring at 80 °C for 6 h. The product obtained was washed with deionized water to remove any unreacted hydroxamic acid and dried in the oven at 60 °C for 12 h. ADHX obtained gave a yield of 96% (wt/wt). The reaction scheme is shown in Fig. 1b.

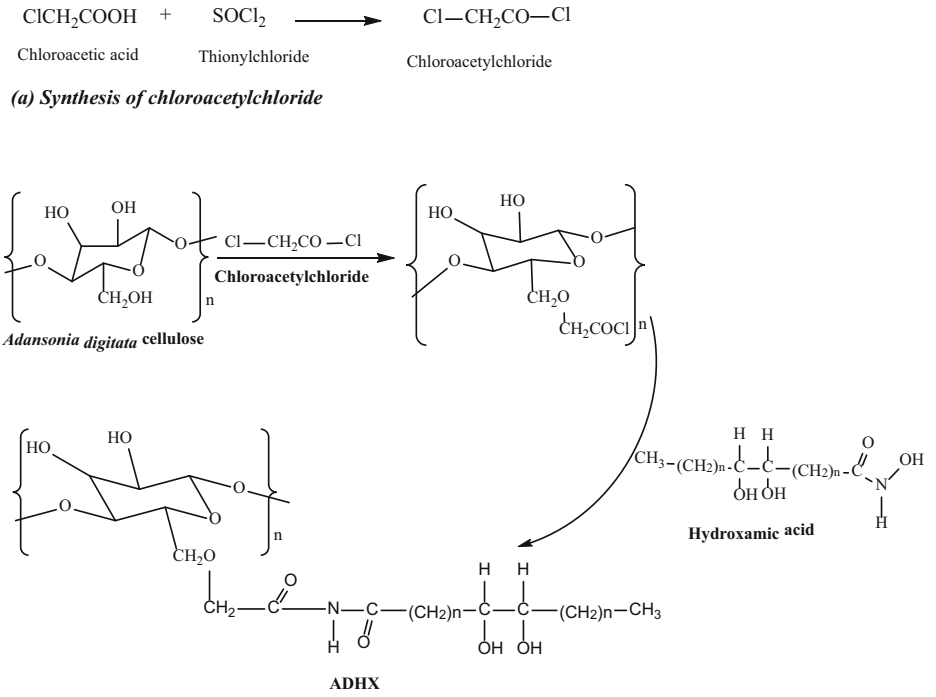


**Fig. 1** (a) Synthesis of chloroacetylchloride, (b) Synthesis of ADHX

## 2.5 Characterization of ADHX

ADHX was blended with KBr, pressed into pellets and subjected to FTIR (FTIR, Perkin Elmer, spectrum RXI 83303) to determine the functional groups it contains. The X-ray diffraction pattern was recorded from 10 to 80 °C of 2θ/s with a scanning speed of 2.00° at 2θ $min^{-1}$ using XRD (7000X-Ray diffractometer, Shimadzu) with filtered Cu Kα radiation operated at 40 kV and 40 mA. The PSD and zeta potential were determined using a zeta potential analyzer (DT1200, Dispersion technology). Thermal stability was monitored via TGA while surface morphology was examined using SEM (JEOL JSM-6360LV, Japan) coupled with EDS (EDS, Thermo Moran, 6714A-ISUS-SN, USA).

## 2.6 Equilibrium Study

Removal of Pb (II) ions by ADHX (0.5 g) was conducted at various time intervals using 100 mL varying concentration of Pb (II) solution (5–100 mg $L^{-1}$) in 250 mL beaker at 298 K and 200 rpm for 170 min. The equilibrium time was established by trying several agitations at 298 K and 200 rpm. During the process of adsorption, clear samples were withdrawn at a different time interval to determine the equilibrium concentration of Pb using Atomic Absorption Spectrometer (Varian AA240FS).

### 2.7 Effect of ADHX Dose, pH and Temperature on Sorption of Pb (II) Ions

Effect of the weight of ADHX on the sorption of Pb (II) ions was determined by varying its weight used during the adsorption process from 0.1 to 1.0 g. To determine the effect of pH on the sorption of Pb (II) ions, 0.5 g of ADHX was used while adjusting the pH (2.7 to 5.8) using 0.1 M HCl and NaOH as appropriate. Furthermore, the effect of temperature on the sorption process was evaluated using 0.5 g of ADHX while varying concentration of Pb (II) ions (5 to 100 mg $L^{-1}$) at different temperatures (303 to 323 K) in 100 mL solution of Pb (II). This was stirred continuously at 200 rpm in a 250 mL beaker for 170 min. Clear samples were withdrawn at a different time interval to determine the equilibrium concentration of Pb using Atomic Absorption Spectrometer (Varian AA240FS).

### 2.8 Desorption Study

Desorption was carried out by weighing 0.5 g of ADHX into 250 mL beaker containing 100 mL solution (100 mg $L^{-1}$) of Pb (II) ions and agitated for 170 min at 298 K. This was filtered and the ADHX-Pb air-dried overnight. The dried ADHX-Pb was poured into a 250 mL beaker containing 100 mL of 0.01 M $NaNO_3$ and agitated for 3 h at 200 rpm and 298 K (Adewuyi and Pereira 2017). The sample was withdrawn at a different time interval and analyzed using Atomic Absorption Spectrometer (Varian AA240FS). Amount of Pb (II) ions desorbed was estimated from the difference between the amount of Pb (II) ions fully loaded on ADHX and the amount of Pb (II) ions in solution.

### 2.9 Quantum Chemical Parameters

Quantum chemical parameters for sorption of Pb (II) ions on ADHX were determined using DFT electronic structure programs at B3LYP/6-31G level theory on Spartan 14.1 software. The molecular electronic structure of ADHX was modelled. This also included the distribution of frontier molecular orbitals in order to establish the reactivity of ADHX with Pb (II) ions as well as its active sites for the sorption.

## 3 Results and Discussion

### 3.1 Synthesis and Characterization of ADHX

The seed of *Adansonia digitata* gave an oil yield of 19.64 ± 0.20% after extraction with n-hexane to defat it. As previously reported (Adewuyi et al. 2019), the fatty acid composition of the extracted oil was determined using Gas Chromatography and was found to contain C18:1 (36.55%) and C18:2 (28.19%) as the most abundant fatty acids. The proton nuclear magnetic resonance (1.1–1.5, 3.4, 3.6 and 7.3 ppm) and FTIR (1665, 1564, 3455 and 1425 $cm^{-1}$) results revealed prominent peaks that confirmed the synthesis of hydroxamic acid just as previously reported (Adewuyi et al. 2019). The FTIR and TGA results of ADHX are presented in Fig. 2. The FTIR spectrum (Fig. 2a) shows a peak at 3370 $cm^{-1}$, which may be attributed to the presence of –OH functional group. The peak at 2835 and 2962 $cm^{-1}$ is attributed to the $CH_2$ and $CH_3$ of alkane from the modifying agent (hydroxamic acid). The peaks at 1560 and 1660 $cm^{-1}$ are assigned to the bending of the CNH group and carbonyl group, respectively.

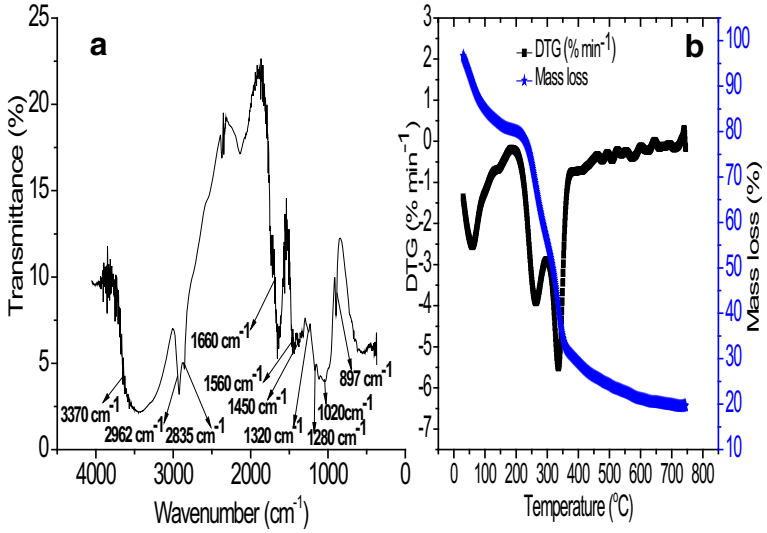


**Fig. 2** (a) FTIR spectrum and, (b) TGA of ADHX

The peak at 1280 $cm^{-1}$ is attributed to C-O stretching of carbonyl functional group while the peak at 1320 $cm^{-1}$ accounts for the C-N stretching at the surface of ADHX. The peak at 1020 $cm^{-1}$ may be assigned to the C-O-C pyranose ring stretching of cellulose while the peak at 897 $cm^{-1}$ accounts for as being the stretching at β-(1 → 4) glycosidic linkages. The peak at 1450 $cm^{-1}$ is assigned to the symmetric $CH_2$ bending vibration, which is the crystallinity band (Ciolacu et al. 2011). The FTIR results can be used to calculate the Empirical Crystallinity Index (*ECI*). The *ECI* may be expressed as:

$$ECI\ (\%) = \frac{A_{1450\ cm^{-1}}}{A_{897\ cm^{-1}}} \times 100 \tag{1}$$

The peak at 1450 $cm^{-1}$ is attributed to the crystalline structure of ADHX while the band at 897 $cm^{-1}$ is assigned to the amorphous region of ADHX. The *ECI* value was found to be 58.35%, which is an expression of the degree of order in the structure of ADHX (Poletto et al. 2014). The TGA and DTG curves of ADHX are shown in Fig. 2b. ADHX exhibited four distinct stages of mass loss during decomposition; however, the previous study has revealed cellulose to decompose mainly by dehydration, depolymerization and glucosan formation (Chauhan et al. 1999), and the observed extra stage might be due to the modification by hydroxamic acid. The curve from the TGA reveals an initial loss in mass between 50 °C and 120 °C, which may be attributed to the loss of water molecules in ADHX. A loss in mass is observed in the range 120–180 °C, which may be attributed to the loss of volatile compounds within the temperature range. This loss might also be considered as being due to the loss of internally bonded water molecules as a result of the ionic interaction around ADHX molecules. A large loss in mass was observed above 180 °C in the range 180–350 °C, which was considered as being the degradation leading to 1,4 and 1,6 anhydroglucopyranoside and depolymerization at 1,4 glycosidic bond (Sharma 2012). The fourth stage of mass loss at temperature above 350 °C may be considered as being pyrolysis to lower molecules.

The X-ray diffraction pattern of ADHX was achieved on X-ray diffractogram, the result is presented in Fig. 3a. The peaks at around 18° and 22.5° 2θ angles are attributed to the diffraction planes of (110) and (002) (Lu et al. 2013). The crystallinity index was calculated as 59.10% from the expression:

$$I_c(\%) = \left(\frac{I_{002} - I_{AM}}{I_{002}}\right) \times 100 \quad (2)$$

using the height of (002) peaks ($I_{002}$, 2θ = 22.5°) and the minimum intensity between the (002) and (110) peaks ($I_{AM}$, 2θ = 18°) where $I_{002}$ represents both crystalline and amorphous material. $I_{AM}$ represents the amorphous material only. Both *ECI* (from FTIR) and $I_c$ (XRD) measures the crystallinity of materials. In this study, crystallinity of ADHX was measured comparing both techniques (FTIR and XRD). Previous studies have shown that although FTIR technique is much simpler, it only measures relative heights or areas, which gives only a relative value because the spectrum contains contribution from both the crystalline and the amorphous region (Åkerholm et al. 2004; Park et al. 2010). However, on measuring the crystallinity of ADHX, the value obtained for the *ECI* (58.35%) relates closely to the $I_c$ (59.10%). The zeta potential is shown in Fig. 3b. The values obtained increased as the pH increased but slightly reduced at pH 5 and 6. However, there was a sharp rise in the value of the zeta potential at pH 8.8 but dropped at pH 9.2, this picked up again as pH increased, although the zeta potential later reduced again with an increase in pH. The lowest zeta potential value was obtained at pH 1.5 and the highest value was obtained at pH 12.1. This value of zeta potential helps in understanding the charges that exist at the surface of ADHX, which guides in finding the most suitable operating pH for the sorption of Pb (II) ions from solution since the zeta potential value helps in knowing the stability and electrostatic repulsion with surrounding particles (Hanaor et al. 2012). The obtained result shows that ADHX is stable in a liquid medium within the studied pH range, which suggests its suitability for solid-liquid interaction, and in this case, the removal of Pb (II) ions in solution. The particle size distribution is presented in Fig. 4a. The distribution of the particles of ADHX is monomodal with the mean distribution size being 10.22 μm. The SEM is shown in Fig. 4b. The surface looks homogeneous with compact structure, which appears rough.

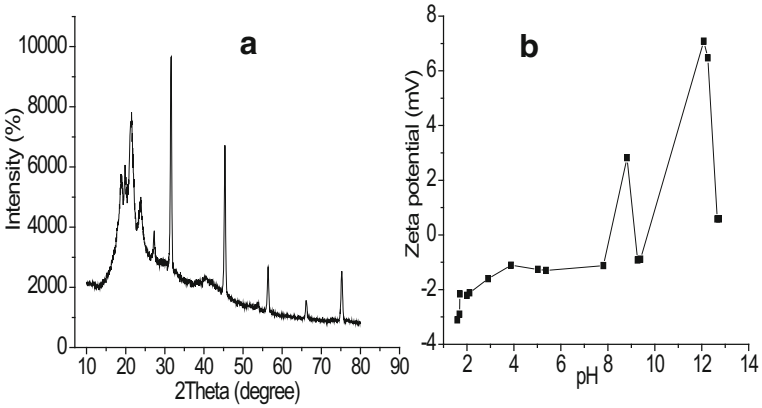


**Fig. 3** (a) XRD and, (b) zeta potential of ADHX

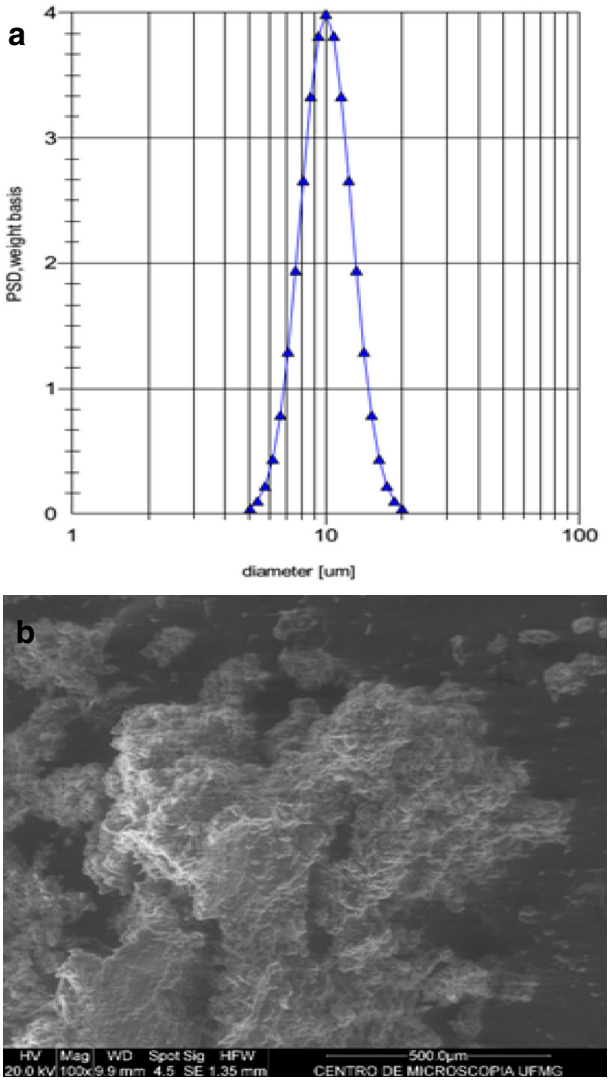


**Fig. 4** (a) Particle size distribution and, (b) SEM of ADHX

### 3.2 Adsorption Process

At the initial stage, this study compared the adsorption capacity of *Adansonia digitata* cellulose (10.30 mg $g^{-1}$) with ADHX (18.00 mg $g^{-1}$) as well as their Pb (II) ion percentage removal. The percentage removal of Pb (II) ions increased from 68.32% (*Adansonia digitata* cellulose) to 89.46% (ADHX). The initial comparison revealed that there was an improvement in the adsorption capacity and percent removal when the *Adansonia digitata* cellulose was modified with hydroxamic acid. Therefore, this study focused more on understanding the use and efficiency of ADHX as a means of removing Pb (II) ions from water. The adsorption of Pb (II) ions from solution by ADHX was studied over a time interval of 170 min. The study showed that ADHX can remove Pb (II) ions from solution as shown in Fig. 5. The EDX result

(Fig. 5a) confirmed the presence of Pb (II) ions at the surface of ADHX after the adsorption process. The SEM image further supported this observation as shown in Fig. 5b. The percentage removal of Pb (II) ions from solution is shown in Fig. 6a while the adsorption capacity exhibited by ADHX towards Pb (II) ions is shown in Fig. 6b. The adsorption capacity of ADHX towards Pb (II) ions was calculated as:

$$q_e = \frac{(C_o - C_e)}{M} V \tag{3}$$

where, $C_o$ and $C_e$ are the initial and final concentrations (mg $L^{-1}$) of Pb (II) ions in solution, respectively. $M$ represents the mass (g) of ADHX, $V$ stands for the volume (L) of Pb (II) ion solution and $q_e$ (mg $g^{-1}$) represents the adsorption capacity of ADHX. The adsorption capacity of ADHX for the removal of Pb (II) ions at 100 mg $L^{-1}$ was 18.00 mg $g^{-1}$. The adsorption capacity of ADHX for the removal of Pb (II) ions from solution increased with time and achieved equilibrium after 100 min. The capacity of ADHX to remove Pb (II) ions from solution also increased as the concentrations of Pb (II) ion increased from 5 to 100 mg $L^{-1}$. This affirms the claim that the initial concentration of adsorbate is important in mass transfer resistance between the adsorbate solution and solid-phase interaction (Rafatullah et al. 2009). The percentage removal also followed a similar trend like the adsorption capacity, this also increased with time and with concentrations of Pb (II) ions. A maximum of 89.46% removal was attained by ADHX for the removal of Pb (II) ions, which reached equilibrium after 100 min.

The effect of pH on the removal of Pb (II) ions from solution is shown in Fig. 7a. The pH of the solution was not allowed to go beyond 6 to prevent Pb from precipitating out of solution. It became obvious that the adsorption capacity of ADHX towards Pb (II) ions in solution, as well as the percentage removal of Pb (II) ions from solution by ADHX, increased as the pH of solution increased. This indicates that the surface of ADHX became more readily available for interaction with Pb (II) ions as pH increased. This suggests that the surface of ADHX must have become negatively charged as pH increased, just as the

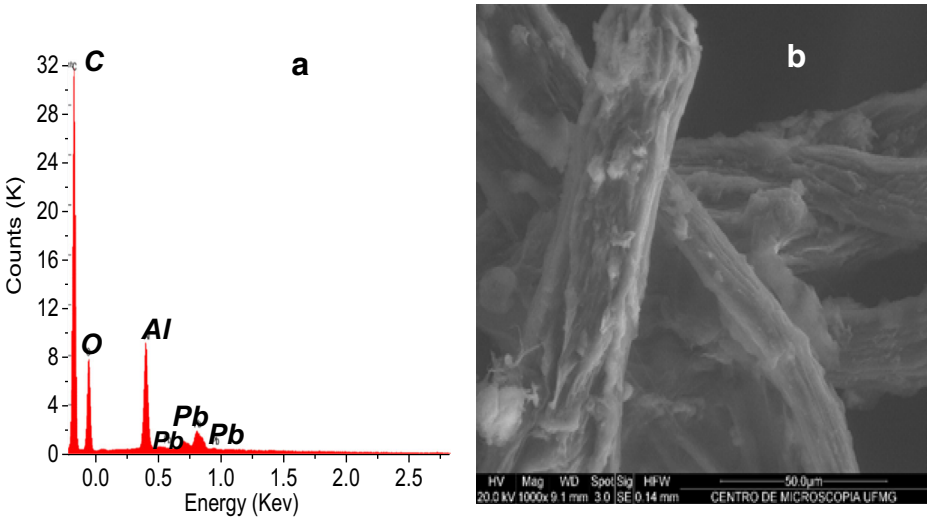


**Fig. 5** (a) EDX and (b) SEM showing surface of ADHX after adsorption

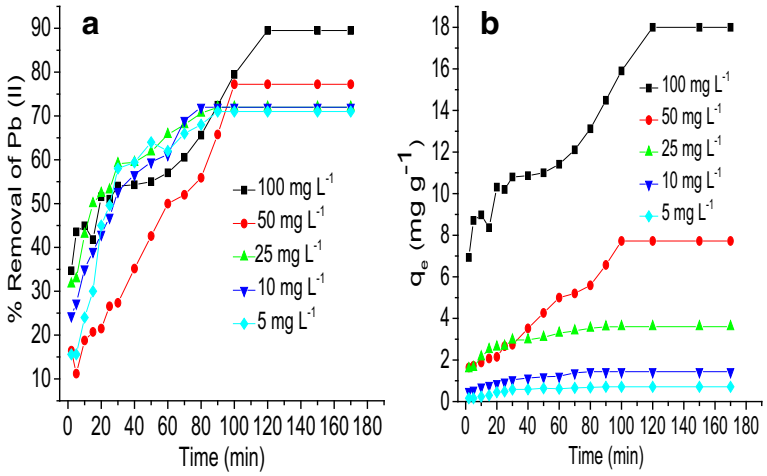


**Fig. 6** (a) Percent removal of $Pb^{2+}$; and (b) $q_e$ of ADHX at different times

zeta potential increased with increase in pH. The removal of Pb (II) ions from solution may have been promoted via ionic interaction. This may have resulted in a complexation reaction between the heteroatoms (Nitrogen and oxygen) at the surface of ADHX and the Pb (II) ions in solution as described in Fig. 8. The lone pair of an electron from the heteroatoms may have driven the interaction as the surface of ADHX may have become less electropositive as pH increased. The effect of the weight of ADHX on the adsorption capacity and percentage removal of Pb (II) ions from solution is described in Fig. 7b. The percent removal increased with an increase in weight of ADHX whereas the adsorption capacity increased with a reduction in weight of ADHX. The observed increase in percent removal with an increase in weight of ADHX may be due to the increase in the availability of the active site for interaction with Pb (II) ions in solution. As weight increased from 0.1 to 1.0 g, the surface must have increased with the possibility of more active sites being available for ionic complexation with Pb (II) ions. However, the observed reduction in adsorption capacity with an increase in weight of ADHX may he explained in terms of mass transfer between the Pb (II) ions in solution and surface of ADHX as weight increased. This suggests an ineffective mass transfer of Pb (II) ions over the surface of ADHX as weight increased. It became obvious that the availability of effective sites for adsorption of Pb (II) ions was hampered or the ratio of effective sites for removal of Pb (II) ions to an ineffective site is small. This means that although the percent removal increased with an increase in the active site as weight increased, the number of active sites available is smaller compared to the ineffective site. This is an indication that the ratio of weight of ADHX to solution volume plays an important role in the sorption of Pb (II) ions.

### 3.3 Kinetic Studies

Sorption of Pb (II) ions by ADHX was studied by fitting data kinetically for pseudo-first-order, pseudo-second-order, intra-particle diffusion, elovich and liquid film diffusion equations. The linearized form of pseudo-first-order equation is given as:

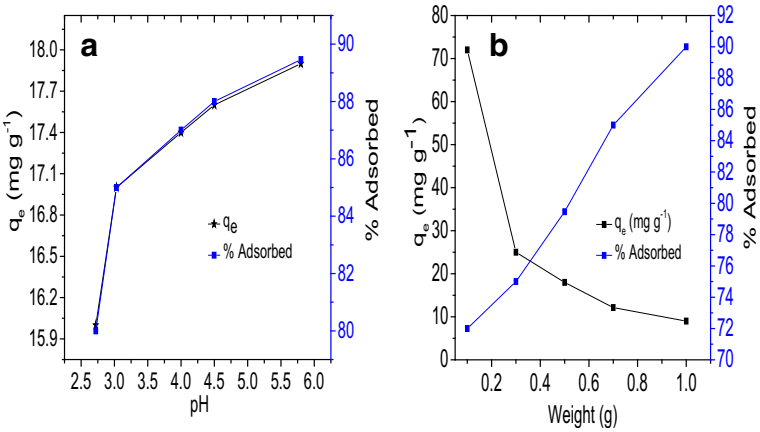


**Fig. 7** Effect of pH (a) and adsorbent weight (b) on percentage adsorption and $q_e$ of ADHX

$$ln(q_e - q_t) = lnq_e - k_1 t \tag{4}$$

where $t$ is time, $q_e$ and $q_t$ are the concentrations of Pb (II) ions at equilibrium and time $t$, respectively, and $k_1$ represents the pseudo-first-order rate constant (min$^{-1}$). To estimate $k_1$, the

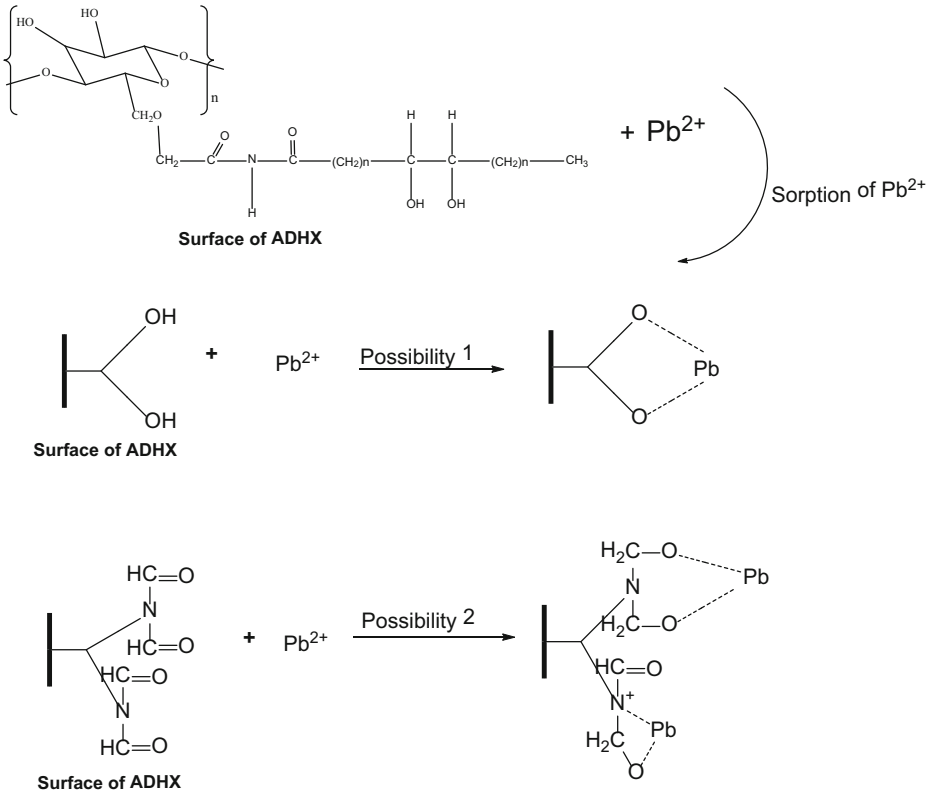


**Fig. 8** Complexation mechanism for the removal of Pb (II) ions from solution by ADHX

pseudo-first-order, $ln(q_e\text{-}q_t)$ was plotted against time $t$ from which $k_1$ and $q_e$ were obtained from the intercept and slope of the plot, respectively. The data did not fit well for pseudo-first-order equation with $R^2$ value 0.846 (Table 1). The data was fitted for pseudo-second-order equation using a linearized expression as:

$$\frac{t}{q_t} = \frac{1}{k_2\, q_e^2} + \frac{t}{q_e} \tag{5}$$

From Eq. (5), $k_2$ (g mg$^{-1}$ min$^{-1}$) represents the adsorption rate constant. The $q_e$, h (initial sorption rate) and $k_2$ were obtained from the slope and intercept of the plot of $t/q_t$ versus $t$. The data fitted well for pseudo-second-order with good regression coefficient (0.944) when compared to the pseudo-first-order (0.846). The $q_e$ for the pseudo-second-order was found to be 19.194 mg g$^{-1}$, and this value is close to the value (18.000 mg g$^{-1}$) obtained from the experimental data. This suggests that the pseudo-second-order model describes the process better than the first-order-model, which suggests the adsorption process to be chemically rate controlled suggesting a chemisorption process. The data were further fitted for intra-particle diffusion model to understand the sorption rate-limiting step. This was achieved as follows:

$$q_t = K_{id}\, t^{0.5} + C \tag{6}$$

In Eq. (6), $C$ (mg g$^{-1}$) is the constant that expresses the thickness of the boundary layer, and $K_{id}$ represents the intra-particle diffusion rate constant (mg g$^{-1}$ min$^{-1/2}$). The plot of $q_t$ versus $t^{1/2}$ gave a straight line with $R^2$ value of 0.949, which indicates that the removal of Pb (II) ions was also controlled by intra-particle diffusion. $C$ and $K_{id}$ values were obtained from the intercept and slope, respectively. However, the regression of the plot did not pass through the origin, which suggests that intra-particle diffusion could not have been the sole rate-limiting step during the sorption of Pb (II) ions by ADHX. Due to this, data were further subjected to a liquid film diffusion model, as described as follows:

$$\ln(1-F) = -K_{fd}\, t \tag{7}$$

**Table 1** Kinetic model parameters for the sorption of Pb (II) ion on ADHX

| Model | Parameter | ADHX |
|---|---|---|
| Pseudo-first-order | $q_e$ (mg g$^{-1}$) | 11.094 |
| | $K_1$ (min$^{-1}$) | 0.012 |
| | $R^2$ | 0.846 |
| Pseudo-second-order | $q_e$ (mg g$^{-1}$) | 19.194 |
| | $K_2$ (g mg$^{-1}$ min$^{-1}$) | 0.002 |
| | $R^2$ | 0.944 |
| | h (mg g$^{-1}$ min) | 0.883 |
| Intra-particle diffusion | $K_{id}$ (mg g$^{-1}$ min$^{1/2}$) | 0.066 |
| | $C$ (mg g$^{-1}$) | 15.152 |
| | $R^2$ | 0.949 |
| Elovich | $\beta$ (g mg$^{-1}$) | 0.396 |
| | $\alpha$ (mg g$^{-1}$ min$^{-1}$) | 0.267 |
| | $R^2$ | 0.781 |
| Liquid film diffusion | $K_{fd}$ | 0.019 |
| | $R^2$ | 0.900 |
| Experiment | $q_e$ (mg g$^{-1}$) | 18.000 |

where F is the fractional attainment of equilibrium given as $q_e/q_t$ and $K_{fd}$ is the adsorption rate constant. To estimate this, −ln(1-F) was plotted against *t*. The $R^2$ value was found to be 0.900, which further corroborate the fact that film diffusion must have played a role in the rate-limiting step. To further probe the possibility of chemical sorption, the data obtained were treated for Elovich model using its linearized form, as follows:

$$q_t = \frac{1}{\beta}\ln(\alpha\beta) + \frac{1}{\beta}\ln t \tag{8}$$

where $\alpha$ is the initial adsorption rate (mg $g^{-1}$ min), and $\beta$ is the extent of surface coverage (g $mg^{-1}$). The $R^2$ value for the plot of $q_t$ vs *lnt* was found to be 0.781. $\alpha$ and $\beta$ were determined from the intercept and slope of the plot.

### 3.4 Isotherms

Data generated for the sorption of Pb (II) ions on ADHX were subjected to Temkin, Langmuir and Freundlich isotherm models. The Temkin model is an important isotherm, which is characterized by the distribution of binding energies up to some maximum binding energy due to ADHX-Pb (II) ions interactions. The model can be expressed as:

$$q_e = \left(\frac{R\,T}{b}\right) ln(AC_e) \tag{9}$$

$$q_e = B\,\ln A + B\,\ln C_e \tag{10}$$

where *A* (L $g^{-1}$) represents the Temkin isotherm equilibrium binding constant, *B* (J $mol^{-1}$) = R T/b, and *b* is the Temkin constant. *T* (K) is the absolute temperature and *R* (8.314 J $mol^{-1}$ K) is the gas constant. On plotting $q_e$ against $lnC_e$, a straight line with $R^2$ value of 0.997 was obtained from which B and A were estimated from the slope and intercept (Table 2).

The Langmuir adsorption isotherm was used to describe the performance of ADHX based on the assumption that the uptake of Pb (II) ions takes place on the homogenous surface by monolayer sorption without interaction between the molecules of Pb (II) ions. The linear equation for the Langmuir isotherm model is given as:

$$\frac{C_e}{q_e} = \frac{1}{Q_o}C_e + \frac{1}{K_L}Q_o \tag{11}$$

The equilibrium amount of Pb (II) ions is represented as $C_e$ (mg $L^{-1}$), $q_e$ (mg $g^{-1}$) represents the amount of Pb (II) ions removed at equilibrium, $Q_o$ (mg $g^{-1}$) is the maximum monolayer coverage capacity, and $K_L$ (L $mg^{-1}$) represents the Langmuir isotherm constant. On plotting $C_e/q_e$ vs $C_e$, a straight line was obtained having a slope of $1/Q_o$, and an intercept of $\frac{1}{K_L}Q_o$ where $K_L$ represents the essential features of the Langmuir isotherm, described by:

$$R_L = \frac{1}{1 + K_L\,C_o} \tag{12}$$

where $C_e$ (mg $L^{-1}$) is the equilibrium concentration of adsorbate, $q_e$ (mg $g^{-1}$) is the amount of metal adsorbed at equilibrium, $Q_o$ (mg $g^{-1}$) is the maximum monolayer coverage capacity, and $K_L$ (L $mg^{-1}$) is the Langmuir isotherm constant. The values of $Q_o$ and $K_L$ were obtained from

**Table 2** Pb (II) ion sorption parameters for Temkin, Langmuir and Freundlich models

| Isotherm | ADHX |
|---|---|
| Temkin | |
| $A$ (L g$^{-1}$) | 11.638 |
| $B$ (J mol$^{-1}$) | 35.301 |
| $b$ | 70.184 |
| $R^2$ | 0.977 |
| Langmuir | |
| $Q_o$ (mg g$^{-1}$) | 18.018 |
| $K_L$ (L mg$^{-1}$) | 138.750 |
| $R^2$ | 1.000 |
| $R_L$ | $7.206 \times 10^{-5}$ |
| Freundlich | |
| $K_f$ (L mg$^{-1}$) | 1.623 |
| $1/n$ | 0.997 |
| 2 | 1.000 |

the slope and intercept of the Langmuir plot. From Eq. (12), $C_o$ represents the initial concentration of Pb (II) ions, and $K_L$ is the Langmuir constant, which relates to the energy of adsorption. The value of $R_L$ is very important and can be interpreted as: when $R_L > 1$, the adsorption process is considered to be unfavourable; the process is considered linear if $R_L = 1$; the process is favourable if $0 < R_L < 1$; and it is irreversible if $R_L = 0$. For the sorption of Pb (II) ions on ADHX, $R_L$ was found to be $7.206 \times 10^{-5}$ which suggests that the process is favourable ($0 < R_L < 1$). This also shows that the sorption of Pb (II) ions on ADHX occurred on a homogenous surface and it is a monolayer sorption with an $R^2$ value of 1.000, which supports the feasibility of the process. The maximum monolayer coverage capacity $Q_o$ was found to be 18.018 mg g$^{-1}$; this value is similar to the adsorption capacity values obtained from the experimental data. The $K_L$ was found to be 138.750 L mg$^{-1}$. This high magnitude of $K_L$ suggests a high heat of sorption, and thus, a strong bond is formed at the surface of ADHX due to the interaction between ADHX and Pb (II) ions. The Freundlich isotherm is an important model that can be used to describe the sorption process. It describes the adsorption process on the heterogeneous surface as an exponential distribution of active sites and their energies (Ayawei et al. 2015), which can be considered as multilayer sorption. It is expressed as:

$$q_e = K_f\, C_e^n \tag{13}$$

where $q_e$ (mg g$^{-1}$) is the amount of Pb (II) ions adsorbed at equilibrium on ADHX, $K_f$ (mg g$^{-1}$) represents the Freundlich isotherm constant, $n$ is the adsorption intensity, and $C_e$ (mg L$^{-1}$) is the equilibrium concentration of Pb (II) ions. The plot of $lnC_e$ against $lnq_e$ gave a straight line with $R^2$ value of 1.000. This is an indication of surface heterogeneity of ADHX suggesting that the surface of ADHX is heterogeneous in its approach for the sorption of Pb (II) ions. $1/n$, as shown in Table 2, is a parameter that reflects the adsorption strength. When $1/n = 1$, then it means that the process is independent of the concentration of Pb (II) ions; when $1/n < 1$, then the sorption is normal; and $1/n > 1$ shows a cooperative adsorption process. The sorption of Pb (II) ions on ADHX had a value of 0.997 for $1/n$, which shows that the process is a normal adsorption process. When the value of $1/n$ is small, the heterogeneity becomes more feasible (Goldberg

2005); during the sorption of Pb (II) ions on ADHX, the value was close to unit (1) which suggests less feasibility.

### 3.5 Thermodynamics of Adsorption

The removal of Pb (II) ions from solution was thermodynamically evaluated from its experimental data obtained from the effect of temperature on the adsorption process. Data were processed to determine thermodynamic parameters such as Gibb's free energy change ($\Delta G^o$), enthalpy change ($\Delta H^o$) and entropy change ($\Delta S^o$). The adsorption equilibrium constant $b_o$ was estimated from the expression (Ekpete et al. 2012):

$$b_o = \frac{C_e}{C_o} \tag{14}$$

$$\Delta G^o = -R\ T\ lnb_o \tag{15}$$

$$\Delta G^o = \Delta H^o - T\Delta S^o \tag{16}$$

In Eq. (14), $C_o$ and $C_e$ are initial and equilibrium amounts of Pb (II) ions. In Eq. (15), $R$ is the universal gas constant (8.314 J $mol^{-1}$ $K^{-1}$) while $T$ (K) is the absolute temperature. A straight line was obtained on plotting $lnb_o$ against the reciprocal of temperature (1/T) to determine $\Delta H^o$ and $\Delta S^o$ from the slope and intercept. The values for $\Delta G^o$ and $q_e$ obtained at different temperatures are presented in Table 3. The values for both $\Delta G^o$ and $q_e$ increased as temperature increased from 303 to 323 K. The highest $\Delta G^o$ value obtained was 0.540 kJ $mol^{-1}$ $K^{-1}$ while the least was 0.507 kJ $mol^{-1}$ $K^{-1}$. The value is positive, which is an indication that the process is non-spontaneous. The adsorption capacity also increased from 18.00 to 19.60 mg $g^{-1}$. The values for $\Delta H^o$ and $\Delta S^o$ are presented in Table 4. The negative nature of enthalpy shows that the process is exothermic while the negative nature of entropy suggests that the process is well ordered indicating a stable configuration of Pb (II) ions on the surface of ADHX.

The parameters obtained for the sorption of Pb (II) ions on ADHX was compared with other biosorbents found in literature as presented in Table 5. Values obtained for ADHX compared favourably with previously reported biosorbents. The adsorption capacity compared better than other plant-sourced biosorbents reported except in the case of *Ficus benghalensis* (Nagpal and Rezaei 2010; Surisetty et al. 2013), activated carbon (Salihi et al. 2017) and Peanut shells (Taşar and Özer 2020). The adsorption isotherm reported for most of the biosorbent was Langmuir isotherm while sorption of Pb (II) ions on ADHX favours Langmuir, Temkin and Freundlich, isotherm models. The $\Delta G^o_{ads}$ value for ADHX was positive while for other reported biosorbents was negative, which suggests the current process to be non-

**Table 3** $\Delta G$ and $q_e$ obtained at various temperatures

| ADHX | | | | | |
|---|---|---|---|---|---|
| $T$ (K) | 303 | 308 | 313 | 318 | 323 |
| $q_e$ (mg $g^{-1}$) | 18.00 | 18.10 | 18.40 | 19.00 | 19.60 |
| $\Delta G$ (kJ $mol^{-1}$ $K^{-1}$) | 0.507 | 0.515 | 0.523 | 0.532 | 0.540 |

**Table 4** Thermodynamic parameters obtained from plot of $lnb_o$ vs $1/T$ for sorption of Pb (II) by ADHX

| Parameters | ADHX |
|---|---|
| $\Delta H$ (kJ mol$^{-1}$) | −69.774 |
| $\Delta S$ (kJ mol$^{-1}$ K$^{-1}$) | −0.214 |

spontaneous. However, ADHX has a negative $\Delta S^o_{ads}$ value while other reported biosorbents showed a positive value, which suggests the suitability of ADHX over other reported materials as this indicates the formation of a stable configuration of Pb (II) ions on the surface of ADHX.

### 3.6 Desorption

The desorption study was conducted to evaluate the economic viability of ADHX. This includes its regeneration capacity and how it can be reused over time. This also helps to check and control the disposal of ADHX after use. Mostly, this guides on the recovery of Pb (II) after it had been adsorbed by ADHX, which means it can be regained and reused. Desorption of Pb (II) ions from the surface of ADHX was calculated as:

$$Desorption\ (\%) = \frac{q_e(desorption)}{q_e(adsorption)} \times 100 \tag{17}$$

During this study, a desorption capacity of 68.75% was attained for the removal of Pb (II) ions from the surface of ADHX. This suggests that Pb (II) ions may probably be chemically bonded to the surface of ADHX. Moreover, the kinetic and isotherm models pointed towards chemisorption as the adsorption mechanism with the $\Delta S^o$ suggesting a well-ordered and stable configuration of Pb (II) ions on the surface of ADHX, a configuration or bond which might not be easily broken.

### 3.7 Quantum Chemical Computations

Sorption of Pb (II) ions by ADHX may be described by ionic interaction between the surface of ADHX and Pb (II) ions in solution. This interaction may have occurred as described in Fig. 8. However, this interaction could have resulted in the formation of strong bonds, which could probably account for the 68.75% desorption obtained. Nonetheless, this interaction was further viewed using DFT at B3LYP/6-31G level theory using Spartan 14.1 software as previously described (Adewuyi et al. 2019; Adewuyi and Oderinde 2019). Fig. 9 shows the electronic properties of ADHX, which includes the optimized geometry, highest occupied molecular orbital (HOMO) and lowest unoccupied molecular orbital (LUMO) density distribution, electron density, electrostatic potential map, local ionization potential map, Mulliken charge and electrostatic charges of ADHX. The presence of oxygen and nitrogen atoms in the molecular structure of ADHX as revealed by the optimized geometry suggests the presence of non-bonding electrons in ADHX, which may participate in chemical bonding, thus adsorption interaction. Presence of non-bonding electrons in the molecules is indicative of electronegative sites, which is further corroborated with the exhibition of negative Mulliken charges as well as negative electrostatic charges as shown in Fig. 9. This showed that ADHX can exhibit nucleophilic characters towards Pb (II) ions. The negative charges are indications that

**Table 5** Comparison of the adsorption of Pb (II) ions on ADHX with other biosorbents in literature

| Material | $q_e$ (mg $g^{-1}$) | Adsorption isotherm | $\Delta G^o_{ads}$ (kJ $mol^{-1}$) | $\Delta H^o_{ads}$ (kJ $mol^{-1}$) | $\Delta S^o_{ads}$ (J $mol^{-1}$ $K^{-1}$) | Mechanism | Reference |
|---|---|---|---|---|---|---|---|
| *Dacryodes edulis* | 10.42 | Freundlich | – | – | – | Chemisorption | Overah and Odiachi (2017) |
| *Ficus benghalensis* | 19.34 | Langmuir | – | – | – | Ion exchange | Nagpal and Rezaei (2010) |
| Cedar leaf ash | 7.23 | Langmuir | – | – | – | – | Salihi et al. (2017) |
| Activated carbon | 23.40 | Langmuir | – | – | – | – | Salihi et al. (2017) |
| *Ficus benghalensis* | 28.63 | Langmuir | – | – | – | Chemisorption | Surisetty et al. (2013) |
| Corncob | 3.30 | Freundlich | - 17.43 | 25.05 | 135.48 | Ion exchange | Mengistie et al. (2008) |
| Peanut shells | 56.50 | Langmuir | −24.69 | −15.46 | 0.315 | Chemisorption | Taşar and Özer (2020) |
| Beans husk | 12.64 | Langmuir | −0.587 | 72.500 | 0.234 | Chemisorption | Onwordi et al. (2019) |
| Fish scale | 11.49 | Temkin | −8.159 | 8.800 | 0.057 | Chemisorption | |
| Activated carbon | 14.01 | Langmuir | – | – | – | – | Liu et al. (2020) |
| Peanut shell | 9.50 | Langmuir | – | – | – | – | |
| Sawdust | 5.50 | Langmuir | – | – | – | – | |
| Banana pith | 11.00 | Langmuir & Freundlich | – | – | – | Chemisorption | Kakoi et al. (2016) |
| Mineral | 9.91 | – | −10.612 | 12.360 | 0.171 | Chemisorption | Cruz-Olivares et al. (2016) |
| HPAL | 12.66 | Freundlich | −3.502 | 9.27 | 0.050 | Physisorption & Chemisorption | Wanga et al. (2018) |
| PAL | 10.83 | Freundlich | −3.073 | 21.68 | 0.068 | | |
| ADHX | 18.00 | Langmuir, Temkin & Freundlich | 0.507 | −69.774 | −0.214 | Chemisorption & Ionic interaction | This study |

- = Not reported

HPAL = $HNO_3$-modified *P. Americana*, PAL = *P. americana*

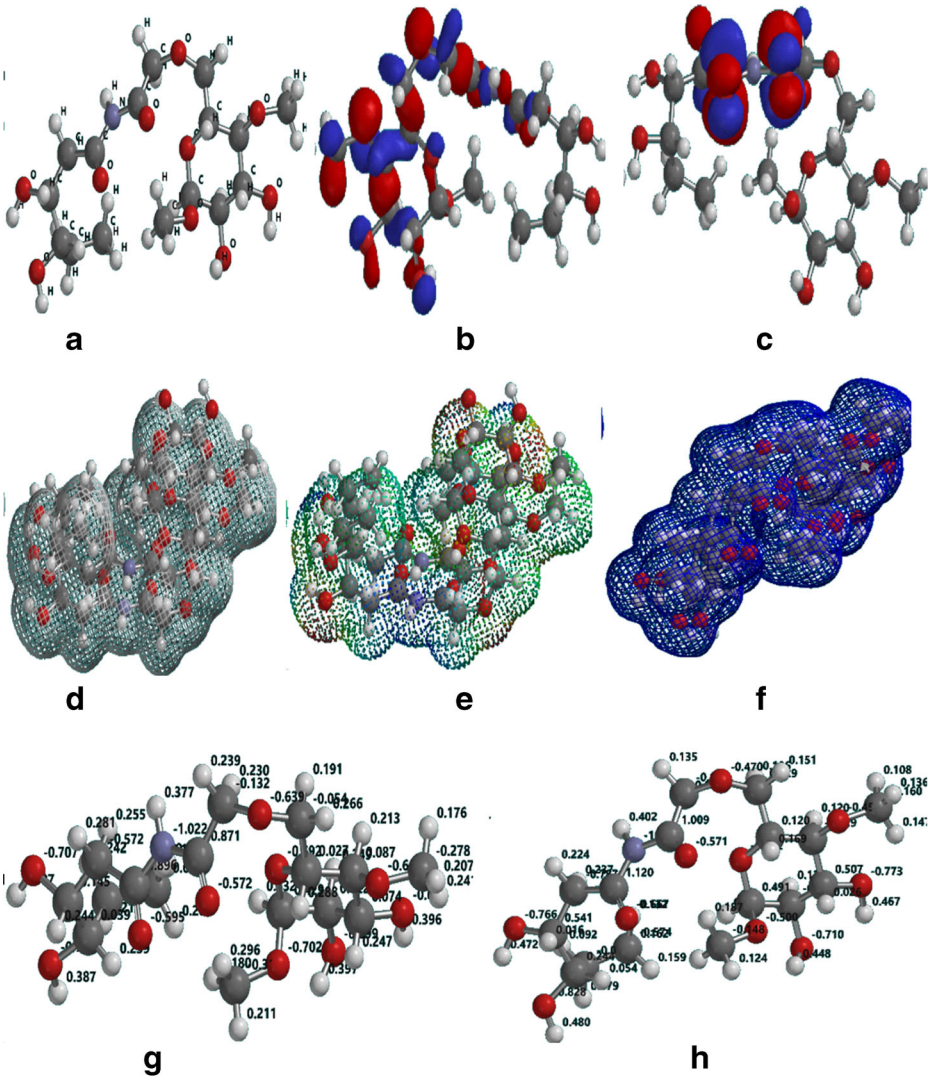


**Fig. 9** Electronic properties of ADHX: Optimized geometry of ADHX (A), HOMO density distribution of ADHX (B); LUMO density distribution of ADHX (C), Electron density of ADHX (D), Electrostatic potential map of ADHX (E), Local ionization potential map of ADHX (F), Mulliken charge of ADHX (G) and Electrostatic charge of ADHX (H)

ADHX tends to donate electrons to the d-orbital of Pb for interaction. Such nucleophilic interaction may have occurred at the HOMO, which represents the site on ADHX with high electron density. This site may probably be the active site for the interaction between ADHX and Pb (II) ions. This interaction may have led to the formation of a strong covalent bond. This also explains the $\Delta S^o$ value, which suggests an ordered and stable configuration of Pb (II) ions surface coverage on ADHX. Table 6 presents the molecular properties exhibited by ADHX. The surface area was found to be 407.60 Å$^2$, the solvation energy was −62.85 kJ mol$^{-1}$ and dipole moment was 4.94 debye. The energy gap ($\Delta E$) was calculated as:

**Table 6** Molecular properties of ADHX calculated using DFT at B3LYP/6-31G basis set level

| Quantum Chemical Property | Value |
|---|---|
| Molecular surface area (Å$^2$) | 407.60 |
| Energy (au) | −1417.92 |
| $E_{HOMO}$ (eV) | −10.70 |
| $E_{LUMO}$ (eV) | 3.82 |
| $E_{LUMO\text{-}HOMO}$ (eV) | 14.52 |
| Dipole moment (debye) | 4.94 |
| Volume (Å$^3$) | 377.13 |
| Solvation energy (kJ mol$^{-1}$) | −62.85 |
| Group | *C1* |
| Polarizability (C$^2$ m N$^{-1}$) | 68.57 |
| η (eV) | 7.26 |

$$\Delta E = E_{LUMO} - E_{HOMO} \tag{18}$$

The value was found to be 14.52 eV. The value is an expression of electronic interaction between ADHX and Pb (II) ions. The lower the value, the better the interaction, and hence, the sorption of Pb (II) ions on ADHX (Adewuyi and Oderinde 2019). The absolute hardness (η) was calculated as:

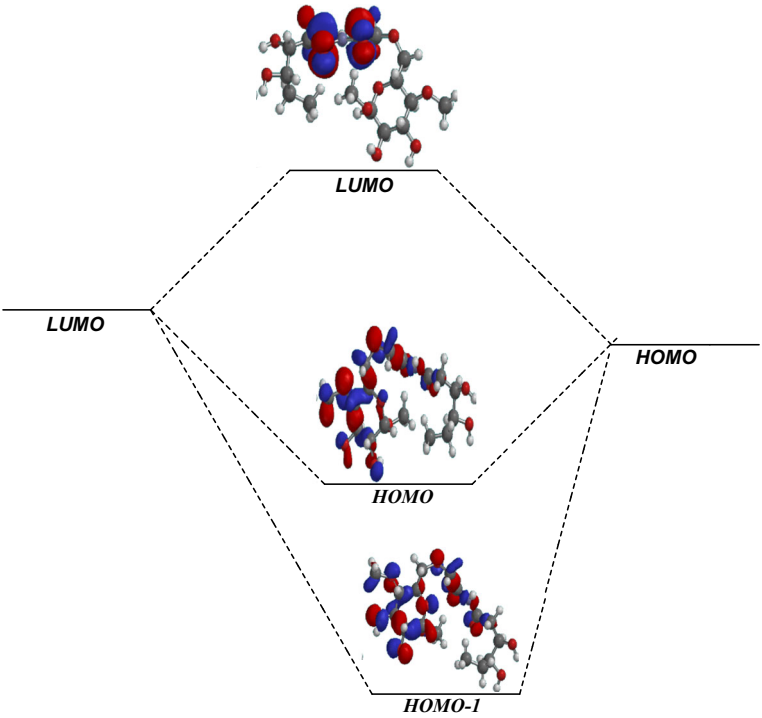


**Fig. 10** Molecular orbitals of ADHX

$$\eta = \frac{E_{LUMO} - E_{HOMO}}{2} \tag{19}$$

Absolute hardness is an expression of the softness of ADHX. Adsorption is expected to take place at soft regions on ADHX. The softer the molecule, the more reactive the molecule becomes and in this case, the better the adsorption process. Figure 10 shows the molecular orbitals of ADHX revealing the HOMO and LUMO electronic interaction, which suggests the mechanism of sorption to be via ionic interaction.

### 3.8 Cost Analysis and Economic Prospect

The cost of removal of Pb (II) ions from solution by ADHX was estimated taking into consideration, process treatment, transportation, energy consumption, maintenance, regeneration, and desorption. With the assumption of a 1 million liters capacity, the cost of treatment ranged between US $8.70 – US $21.50 per million liters. This is cheaper than the report by Daniel et al. (2020), which involved the use of citric acid modified cellulose for the removal of Cr (III) ions. Removal of Pb (II) ions by ADHX is economically feasible compared to techniques such as electrodialysis, electrothermal, reverse osmosis, and advance oxidation, which cost about US $450 per million liters, although the cost of water treatment per million liters is estimated as US $10-US $200 (de Andrade et al. 2018) for biologically sourced materials. As the world population increases, the demand for provision of clean water will also increase. However, the use of adsorption as a means for water treatment remains a viable means through which this may be achieved due to the low cost and ease of process optimization.

## 4 Conclusions

Cellulose isolated from the seed of *Adansonia digidata* was modified with hydroxamic acid (synthesized from the seed of *Adansonia digidata*). The modified cellulose (ADHX) was characterized using FTIR, XRD, SEM, EDX, TG and particle size analyzer. ADHX was also evaluated for its capacity to serve as a resource for the removal of Pb (II) ions in solution. The result from the characterization confirmed the production of ADHX. From the adsorption experiment, ADHX exhibited the capacity to remove Pb (II) ions from solution with an adsorption capacity of 18.00 mg $g^{-1}$ in an adsorption process that is non-spontaneous, exothermic and that obeys Langmuir, Freundlich and Temkin isotherm models. The mechanism for the process is described by chemisorption and ionic interaction with a desorption capacity of 68.75%. The process was also described by quantum chemical computation.

**Acknowledgements** Author is grateful to the Department of Chemistry, Federal University of Minas Gerais, Brazil for use of equipment and provision of research space. Author is also grateful to the International Foundation of Science for awarding a research grant (No W/5401-1).

## Compliance with Ethical Standards

**Conflict of Interest** No Conflict of Interest

## References


Abdeen Z (2015) Enhanced recovery of $Pb^{2+}$ ions from aquatic media by using polyurethane composite as adsorbent. Environ Process 2:189–203

Adewuyi A, Oderinde RA (2019) Chemically modified vermiculite clay: a means to removing emerging contaminant from polluted water system in developing nation. Polym Bull 76:4967–4989

Adewuyi A, Oderinde RA, Fayemi SO (2019) Fatty hydroxamic acid mixture from underutilized *Adansonia digitata* seed oil: A potential means for scavenging free radicals and combating drug resistant microorganisms. La Riv Ital Delle Sost Grasse XCVI:269–284

Adewuyi A, Oderinde RA, Rao BVSK, Prasad RBN, Anjaneyulu B (2012) *Blighia unijugata* and *Luffa cylindrica* seed oils: renewable sources of energy for sustainable development in rural Africa. BioEner Res 5:713–718

Adewuyi A, Pereira FV (2017) Underutilized *Luffa cylindrica* sponge: a local bio-adsorbent for the removal of Pb (II) pollutant from water system. Beni-Suef Uni J Basic Appl Sci 6:118–126

Åkerholm M, Hinterstoisser B, Salmén L (2004) Characterization of the crystalline structure of cellulose using static and dynamic FT-IR spectroscopy. Carbohydr Res 339:569–578

Anyanwu BO, Ezejiofor AN, Igweze ZN, Orisakwe OE (2018) Heavy metal mixture exposure and effects in developing nations: an update. Toxics 6:65

Ayawei N, Ekubo AT, Wankasi D, Dikio ED (2015) Adsorption of Congo red by Ni/Al-$CO_3$: equilibrium, thermodynamic and kinetic studies. Orien J Chem 31:1307–1318

Babu AN, Mohan GVK, Ravindhranath K (2016) Removal of chromium (VI) from polluted waters using adsorbents derived from *Chenopodium album* and *Eclipta prostrate* plant materials. Int J ChemTech Res 9: 506–516

Batmaz R, Mohammed N, Zaman M, Minhas G, Berry R, Tam K (2014) Cellulose nanocrystals as promising adsorbents for the removal of cationic dyes. Cellulose 21:1655–1665

Bolisetty S, Peydayesh M, Mezzenga R (2019) Sustainable technologies for water purification from heavy metals: review and analysis. Chem Soc Rev 48:463–487

Buvaneswaria N, Kannanb C (2011) Plant toxic and non-toxic nature of organic dyes through adsorption mechanism on cellulose surface. J Hazard Mater 189:294–300

Chauhan GS, Bhatt S, Kaur I, Singha AS, Kaith BS (1999) Modification of natural polymers: graft copolymers of methyl methacrylate onto rayon fibre initiated by ceric ions- a study in the swelling and thermal properties. J Polym Mat 16:245–252

Chen G, Shi L (2017) Removal of cd(II) and Pb(II) ions from natural water using a low-cost synthetic mineral: behavior and mechanisms. RSC Adv 7:43445–43454

Choi S, Jeong Y (2008) The removal of heavy metals in aqueous solution by hydroxyapatite/cellulose composite. Fiber Polym 9:267–270

Ciolacu D, Ciolacu F, Popa VI (2011) Amorphous cellulose-structure and characterization. Cellulose Chem Technol 45:13–21

Coelho GF, Gonçalves AC, Schwantes D, Rodríguez EA, Tarley CRT, Dragunski D, Junior EC (2018) Removal of cd(II), Pb(II) and Cr(III) from water using modified residues of *Anacardium occidentale* L. Appl Water Sci 8:96

Cruz-Olivares J, Martínez-Barrera G, Pérez-Alonso C, Barrera-Díaz CE, Chaparro-Mercado MC, Ureña-Núñez F (2016) Adsorption of lead ions from aqueous solutions using gamma irradiated minerals. J Chem 2016:1–7

de Andrade JR, Oliveira MF, da Silva MGC, Vieira MGA (2018) Adsorption of pharmaceuticals from water and wastewater using nonconventional low-cost materials: A Review. Ind Eng Chem Res 57:3103–3127

Daniel AB, Zahir E, Hussain I, Naz S, Asghar MA (2020) Citric acid modified cellulose: a cost effective adsorbent for the immobilization of Cr (III) ions from the aqueous phase. Ener Sourc part a: Recov Utiliz environ effects 1–13. https://doi.org/10.1080/15567036.2020.1773963

Ekpete OA, Horsfall M Jnr, Spiff AI (2012) Kinetics of chlorophenol adsorption onto commercial and fluted pumpkin activated carbon in aqueous systems. Asian J Nat Appl Sci 1:106–117

Escudero-Oñate C, Poch J, Villaescusa I (2017) Adsorption of cu(II), Ni(II), Pb(II) and cd(II) from ternary mixtures: Modelling competitive breakthrough curves and assessment of sensitivity. Environ Process 4:833–849

Flauzino Neto WP, Silvério HA, Dantas NO, Pasquini D (2013) Extraction and characterization of cellulose nanocrystals from agro-industrial residue – soy hulls. Ind Crop Prod 42:480–488
Fox SC, Li B, Xu D, Edgar KJ (2011) Regioselective esterification and etherification of cellulose: a review. Biomacromolecules 12:1956–1972
Galadima A, Garba ZN (2012) Heavy metals pollution in Nigeria: causes and consequences. Elixir Pollut 45: 7917–7922
Galadima A, Muhammad NU, Garba ZN (2010) Spectroscopic investigation of heavy metals in waste water from university students' halls of residence. Int J Chem 20:239–244
Goldberg S (2005) Equations and models describing adsorption processes in soils. Soil science Society of America, USA. Chemical Processes in Soils. SSSA Book Series
Gusain R, Kumar N, Fosso-Kankeu E, Ray SS (2019) Efficient removal of Pb(II) and cd(II) from industrial mine water by a hierarchical $MoS_2$/SH-MWCNT nanocomposite. ACS Omega 4:13922–13935
Hanaor DAH, Michelazzi M, Leonelli C, Sorrell CC (2012) The effects of carboxylic acids on the aqueous dispersion and electrophoretic deposition of $ZrO_2$. J Eur Cer Soc 32:235–244
He Y, Wu P, Xiao W, Li G, Yi J, He Y, Chen C, Ding P, Duan Y (2019) Efficient removal of Pb(II) from aqueous solution by a novel ion imprinted magnetic biosorbent: adsorption kinetics and mechanisms. PLoS One 14:e0213377
Hokkanen S, Bhatnagar A, Sillanpaa M (2016) A review on modification methods to cellulose-based adsorbents to improve adsorption capacity. Water Res 91:156–173
Imran M, Anwar K, Akram M, Shah GM, Ahmad I, Shah NS, Khan ZUH, Rashid MI, Akhtar MN, Ahmad S, Nawaz M, Schotting RJ (2019) Biosorption of Pb(II) from contaminated water onto *Moringa oleifera* biomass: kinetics and equilibrium studies. Int J Phytoremed 21:777–789
Joseph L, MoonJun B, Flora JRV, Park CM, Yoon Y (2019) Removal of heavy metals from water sources in the developing world using low-cost materials: a review. Chemosphere 229:142–159
Kakoi B, Kaluli JW, Ndiba P, Thiong'o G (2016) Removal of lead (II) from aqueous solution using natural materials: a kinetic and equilibrium study. J Sust Res Eng 3:53–62
Koesmawati TA, Moelyo M, Rizqiani A, Tanuwidjaja S (2017) Pre-concentration of Pb, cd, and Ni in river water using back extraction method. IOP Conf. Ser.: earth. Environ Sci 60:012021
Liu X, Xu X, Dong X, Park J (2020) Competitive adsorption of heavy metal ions from aqueous solutions onto activated carbon and agricultural waste materials. Pol J Environ Stud 29:749–761
Lu H, Gui Y, Zheng L, Liu X (2013) Morphological, crystalline, thermal and physicochemical properties of cellulose nanocrystals obtained from sweet potato residue. Food Res Int 50:121–128
Mengistie AA, Rao TS, Rao AVP, Singanan M (2008) Removal of lead (II) ions from aqueous solutions using activated carbon from *Militia ferruginea* plant leaves. Bull Chem Soc Ethiop 22:349–360
Merganpour AM, Nekuonam G, Tomaj OA, Kor Y, Safari H, Karimi K, Kheirabadi V (2015) Efficiency of lead removal from drinking water using cationic resin purolite. Environ Health Eng Manag 2:41–45
Nacke H, Gonçalves AC Jr, Campagnolo MA, Coelho GF, Schwantes D, dos Santos MG, Briesch DL Jr, Zimmermann J (2016) Adsorption of cu (II) and Zn (II) from water by *Jatropha curcas* L. as biosorbent. Open Chem 14:103–117
Nagpal UMAMK, Rezaei H (2010) Equilibrium sorption studies for $Cu^{2+}$ and $Pb^{2+}$ metal ionson three different biomasses. Curr World Environ 5:243–251
Oke IA, Lukman S, Ismail A, Fehintola EO, Amoko JS (2017) Removal of lead ions from water and wastewaters electrochemically. Water Purif Acad Press:643–691
Onwordi CT, Uche CC, Ameh AE, Petrik LF (2019) Comparative study of the adsorption capacity of lead (II) ions onto bean husk and fish scale from aqueous solution. J Water Reuse Desal 9:249–262
Orosun MM, Tchokossa P, Nwankwo LI, Lawal TO, Bello SA, Ige SO (2016) Assessment of heavy metal pollution in drinking water due to mining and smelting activities in Ajaokuta, Nigeria. Nig J Technol Devel 13:31–39
Overah LC, Odiachi I (2017) Evaluation of *Dacryodes edulis* (native pear) seed biomass for Pb (II) sorption from aqueous solution. J Appl Sci Environ Manage 21:186–199
Park S, Baker JO, Himmel ME, Parilla PA, Johnson DK (2010) Cellulose crystallinity index: measurement techniques and their impact on interpreting cellulase performance. Biotechnol Biofuels 3:10
Poletto M, Ornaghi HL Jr, Zattera AJ (2014) Native cellulose: structure, characterization and thermal properties. Materials 7:6105–6119
Rafatullah M, Sulaiman O, Hashim R, Ahmad A (2009) Adsorption of copper (II), chromium (III), nickel (II) and lead (II) ions from aqueous solutions by meranti sawdust. J Hazard Mater 170:969–977
Ravulapalli S, Kunta R (2017) Defluoridation studies using active carbon derived from the barks of *Ficus racemosa* plant. J Fluor Chem 193:58–66
Salihi IU, Kutty SRM, Isa MH (2017) Adsorption of lead ions onto activated carbon derived from sugarcane bagasse. IOP Conf. Ser.: mater Sci Eng 201:012034

Sarkar M, Sarkar S (2017) Adsorption of Cr(VI) on iron(III) cellulose nanocomposite bead. Environ Process 4: 851–871

Sharma RK (2012) A study in thermal properties of graft copolymers of cellulose and methacrylates. Advan Appl Sci Res 3:3961–3969

Surisetty VR, Kozinski J, Nageswara LR (2013) Biosorption of lead ions from aqueous solution using *Ficus benghalensis* L. J Eng 2013:1–8

Taşar S, Özer A (2020) Pb(II) ions using peanut (*Arachis Hypogaea*) shell-based biochar from aqueous media. Pol J Environ Stud 29:293–305

Tenebe IT, Emenike CP, Chukwuka CD (2018) Prevalence of heavy metals and computation of its associated risk in surface water consumed in ado-Odo Ota, south-West Nigeria. Human Ecol Risk Assessment: An Int J 25:882–904

Triantafyllidou S, Edwards M (2012) Lead (Pb) in tap water and in blood: implications for lead exposure in the United States. Crit Rev Environ Sci Technol 42:1297–1352

Wanga G, Zhanga S, Yaoa P, Chena Y, Xua X, Lia T, Gong G (2018) Removal of Pb(II) from aqueous solutions by *Phytolacca americana* L. biomass as a low cost biosorbent. Arab J Chem 11:99–110

Wasike PW, Nawiri MP, Wanyonyi AA (2019) Levels of heavy metals (Pb, Mn, cu and cd) in water from river Kuywa and the adjacent wells. Environ Ecol Res 7:135–138

World Health Organization (2010) Childhood lead poisoning, printed by the WHO document production services. Switzerland, Geneva

Yu X, Tong S, Ge M, Wu L, Zuo J, Cao C, Song W (2013) Adsorption of heavy metal ions from aqueous solution by carboxylated cellulose nanocrystals. J Environ Sci 25:933–943

Zhao D, Yu Y, Chen JP (2016) Treatment of lead contaminated water by a PVDF membrane that is modified by zirconium, phosphate and PVA. Water Res 101:564–573